Magnetoresistance of the double-tunnel-junction Coulomb blockade with magnetic metals

Kingshuk Majumdar and Selman Hershfield
Department of Physics and National High Magnetic Field Laboratory, University of Florida, 215 Williamson Hall, Gainesville, Florida 32611

(Received 18 September 1997)

We have studied the junction magnetoresistance (JMR) and the differential junction magnetoresistance (DJMR) for double tunnel junctions with magnetic metals in the Coulomb blockade regime. Spikes are seen in both the JMR and the DJMR vs voltage curves. They occur at those places where the current increases by a step. In all cases the large bias limit can be obtained by adding the resistances of each of the junctions in series. The JMR is positive in all the cases we studied, whereas the DJMR can be positive or negative as a function of the voltage. Moreover, the relative variation of the DJMR as a function of the voltage is larger than the variation of the JMR with the voltage. [S0163-1829(98)00418-4]

I. INTRODUCTION

Electron tunneling through tunnel junctions which consist of magnetic metals separated by insulators has a long history.[1] Some of the earliest experiments were on tunneling between a superconductor and a ferromagnet (FM).[2] In these experiments, a difference between the spin-up and spin-down density of states of a superconductor in a magnetic field was observed. These experiments also provided a quantitative measure of the spin polarization of the current from the ferromagnetic metal. Later experiments were done on tunneling between two ferromagnetic metals.[3] Because of the spin dependence of the density of states, the conductance changed when the relative orientation of the two magnetizations changed. Tunneling between two ferromagnetic metals has experienced renewed interest because of its potential application in information storage. One of the measurable quantities of practical importance is the junction magnetoresistance, which is defined as the ratio of the change in the conductance from parallel to antiparallel alignment divided by the parallel conductance. A large magnetoresistance response in low magnetic fields has been observed in a variety of tunnel junctions by several groups.[4–14]

Besides spin, electrons carry charge, and at low temperatures in tunnel junctions with small capacitance, the discreteness of electron charge manifests itself through the physics of the Coulomb blockade.[15–20] The transfer of an electron by tunneling between two initially neutral regions of capacitance C increases the electrostatic energy of the system by an amount $e^2/2C$. At low temperatures and small voltages, the tunneling current is suppressed because of the charging energy. This energy barrier is called the Coulomb blockade. The effect of this in a two-junction system is the incremental increase in the current at voltages where it is energetically favorable for an electron to tunnel to the center island. The occurrence of these current steps in the current-voltage characteristics is known as the ''Coulomb staircase.'' Advances in technology have led to a number of new experiments which exhibit the Coulomb blockade phenomenon: granular thin films,[21,22] lithographically patterned tunnel junctions,[23,24] narrow disordered quantum wires,[25,26] scanning tunneling microscopy of small metal droplets,[27] and metal-insulator-metal tunnel junctions with small metal particles embedded in the insulator.[28–31]

Recently there have been experiments where spin-polarized tunneling and the Coulomb blockade have been combined.[32] For example, in discontinuous metal/insulator multilayers consisting of closely spaced ferromagnetic nanoparticles in an insulating matrix, a Coulomb blockade is seen in the current-voltage characteristic at low temperatures. The purpose of this paper is to further study the nonlinear conductances for parallel and antiparallel magnetization alignment for a double junction with magnetic metals in the Coulomb blockade regime.

The organization of the rest of the paper is as follows. In the next section we describe the model and the master equation used. The expressions for the current, the conductance, the differential conductance, and the junction magnetoresistance are then introduced. The results of the calculation are given in the discussion of Sec. III and summarized in Sec. IV.

II. FORMALISM

The experimental realization of a double tunnel junction consists of three metals separated by oxide layers which act as insulators. The two end leads, denoted by left (L) and right (R), are connected to a constant-voltage source V. This double junction can be modeled as a closed-loop electrical circuit with two leaky capacitors of capacitances C_L and C_R connected in series (Fig. 1). The resistances of the junctions, R_L and R_R, are connected in parallel to C_L and C_R, respectively.

Depending on the number of excess electrons, n, in the center metal, the voltage in the central region V_M fluctuates. The voltage drops $[V_L-V_M(n)]$ and $[V_M(n)-V_R]$ across the left and the right junctions are

$$V_L-V_M(n)=\frac{C_R}{C}V+\frac{ne}{C}+V_P, \tag{1}$$

$$V_M(n)-V_R=\frac{C_L}{C}V-\frac{ne}{C}-V_P, \tag{2}$$

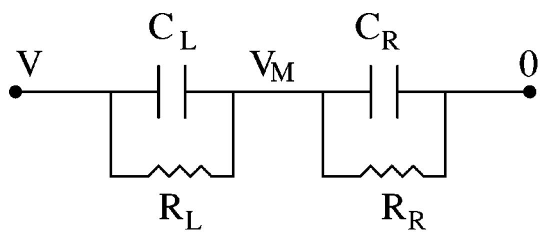

FIG. 1. Schematic diagram of a double-tunnel-junction system. The left and right capacitors (C_L and C_R) are connected in series with a voltage source. The resistances of the left and right junctions are R_L and R_R, respectively. The voltage in the left and right leads is kept fixed at V and 0, whereas in the central region the voltage V_M changes.

where $-e$ is the charge of the electron and C is the capacitance (C_L+C_R). The offset voltage V_P accounts for the fact that even when n and V are zero, V_M may not be zero due to the alignment of the Fermi energy in the middle region. Such effects are seen experimentally[33,34] in a shifting of the I-V characteristic away from a symmetric curve $[I(V)=I(-V)]$. A nonzero V_P can also be created deliberately by patterning a gate capacitor to the central region.[35–37] To describe the transport of electrons we use a semiclassical model.[16,38–40] The different tunneling rates that enter into the dynamics are the rate for electrons to tunnel onto the center metal from the left ($\Gamma^L_{n\to n+1}$) and right ($\Gamma^R_{n\to n+1}$), and the rate for the electrons to leave the center metal to the left ($\Gamma^L_{n\to n-1}$) and right ($\Gamma^R_{n\to n-1}$). These tunnel rates can be calculated using Fermi's golden rule.[38] To express the different tunnel rates in a convenient fashion we introduce a function $\gamma(\epsilon)$:

$$\gamma(\epsilon)=\frac{\epsilon}{1-e^{-\beta\epsilon}}. \tag{3}$$

In terms of the above function the various tunnel rates are

$$\Gamma^{L(R)}_{n\to n\pm 1}=\left(\frac{1}{e^2R_{L(R)}}\right)\gamma\{\pm e[V_M(n)-V_{L(R)}]-E_C\}. \tag{4}$$

Here $E_C=e^2/2C$ is the charging energy, and β is related to the temperature T via $\beta=1/k_BT$. The resistances R_L and R_R depend on the square of a matrix element describing the probability of tunneling through the junction barriers and as well as also on the spin-dependent density of states of the metals.[38] To estimate the junction resistances we will use Julliere's model[3] where for example the parallel G^{P} and antiparallel conductances G^{AP} for a FM/I/FM tunnel junction, where I is an insulator, are given by

$$G^{\mathrm{P}}=\left(\frac{e^2}{h}\right)|T|^2N_1N_2\{a_1a_2+(1-a_1)(1-a_2)\}, \tag{5}$$

$$G^{\mathrm{AP}}=\left(\frac{e^2}{h}\right)|T|^2N_1N_2\{a_1(1-a_2)+(1-a_1)a_2\}. \tag{6}$$

Here the tunneling matrix element T is taken to be both energy and momentum independent. The density of states of the electrons at the Fermi level in the two ferromagnets is N_1 and N_2 and the fraction of the number of spins parallel to the magnetization in the two FM's is a_1 and a_2, respectively. Using the definitions of the spin polarizations P_1 and P_2 of the two FM's,

$$P_1=2a_1-1, \tag{7}$$

$$P_2=2a_2-1. \tag{8}$$

Equations (5) and (6) can be rewritten in terms of P_1 and P_2.

For magnetic materials, there are two types of carriers: majority electrons with spins parallel to the magnetization and minority electrons with spins antiparallel to the magnetization. We make the assumption that the rate of tunneling through the junctions is much smaller than the rate of spin relaxation. Under this assumption the number of majority and minority electrons in the center metal is not conserved separately, but their sum is conserved. This results in a master equation which describes the time evolution of the probability, $\rho_n(t)$, for n excess electrons in the center metal,[16]

$$\frac{d\rho_n(t)}{dt}=[\rho_{n+1}\Gamma_{n+1\to n}-\rho_n\Gamma_{n\to n+1}]-[\rho_n\Gamma_{n\to n-1}-\rho_{n-1}\Gamma_{n-1\to n}], \tag{9}$$

where the net tunnel rate $\Gamma_{i\to j}$ is equal to $(\Gamma^L_{i\to j}+\Gamma^R_{i\to j})$. At steady state, $d\rho_n(t)/dt=0$, the current in the left junction equals the current in the right junction due to current conservation, and is given by

$$I=e\sum_{n=-\infty}^{n=\infty}\rho_n(\Gamma^L_{n\to n-1}-\Gamma^L_{n\to n+1}). \tag{10}$$

To evaluate the current in general, Eqs. (9) and (10) have to be solved numerically. We follow the same procedure described in Ref. 35. At low temperature and voltage, the higher charge states $|n|\gg 1$ are energetically forbidden and therefore we can neglect them. We found that for our choice of parameters it is sufficient to keep the 19 states around $n=0$. The highest and the lowest states are $n=9$ and $n=-9$. The total conductance G is then simply given by dividing the current by the voltage, $G=I/V$, and the differential conductance G_{diff} is obtained by differentiating the current with respect to the voltage, $G_{\mathrm{diff}}=dI/dV$.

There are two possible choice of materials which lead to nonzero magnetoresistance in a two-junction system: (1) all the leads are ferromagnets, i.e., FM/I/FM/I/FM, and (2) the left or the right lead is a paramagnet, i.e., FM/I/FM/I/PM or PM/I/FM/I/FM, where PM is a paramagnet. Note that with the center lead nonmagnetic (FM/I/PM/I/FM) there is no junction magnetoresistance (JMR) or differential junction magnetoresistance (DJMR) because the antiparallel conductance is identical to the parallel conductance within our assumption. For each of these cases, we calculate the conductances for two different relative orientations of the ferromagnet magnetizations: parallel and antiparallel. Here parallel (P) means that the magnetization of all ferromagnets is in the same direction, and antiparallel (AP) means that the magnetization of the center ferromagnetic metal has been reversed. In case (1) of three ferromagnetic metals, other configurations are also possible: the magnetization of the right or the left lead can be reversed, keeping the magnetizations of the other two parallel. For case (2) where one of the left or the right lead is nonmagnetic, the magnetization of right or the left ferromagnetic lead can also be reversed. However, the qualitative features of the current, conductance, and the magnetoresistance curves remain the same. The junction magnetoresistance is then defined as the ratio of the change in the conductance from parallel G^{P} to antiparallel alignments G^{AP}, divided by the parallel conductance,

$$\mathrm{JMR}=1-\frac{G^{\mathrm{AP}}}{G^{\mathrm{P}}}. \tag{11}$$

The differential junction magnetoresistance is defined in the same fashion as the JMR but with the total conductances replaced by the differential conductances G_{diff},

$$\mathrm{DJMR}=1-\frac{G_{\mathrm{diff}}^{\mathrm{AP}}}{G_{\mathrm{diff}}^{\mathrm{P}}}. \tag{12}$$

III. DISCUSSION

The different parameters of our problem are the capacitances C_L and C_R, the parallel resistances R_L^{P} and R_R^{P}, the antiparallel resistances R_L^{AP} and R_R^{AP}, the temperature T, and the offset voltage V_P. To estimate the antiparallel resistances, we use Julliere's model for FM/I/FM tunnel junctions, where the junction magnetoresistance is expressed as a product of the magnitudes of the polarizations of the ferromagnets:[3]

$$\frac{\Delta R}{R^{\mathrm{AP}}}=\frac{2P_1P_2}{(1+P_1P_2)}. \tag{13}$$

In the above equation, ΔR is the change in resistance from antiparallel to parallel orientation, R^{AP} is the junction resistance when the magnetizations of the ferromagnets are antiparallel, and P_1,P_2 are the spin polarizations of the two FM's. Equation (13) can be obtained from Eqs. (5) and (6).

In Fig. 2 the currents and the total conductances are plotted for parallel and antiparallel orientations of the magnetizations. Asymmetric junctions and low temperature are used to obtain the steps in the current. As expected in the Coulomb blockade regime, the current increases by steps [cases (a) and (b)], and the conductance shows oscillations with decreasing amplitude [case (c)]. Case (a) corresponds to a finite offset voltage whereas cases (b) and (c) correspond to zero offset voltage. The effect of a finite V_P is to shift the I-V curves. For convenience we thus take the offset voltage to be zero for our later calculations. Finally, for large enough voltage, the current becomes linear with voltage and the conductance approaches the classical limiting value which is the inverse of the resistance of two resistors connected in series,

$$G=\frac{1}{(R_L+R_R)}. \tag{14}$$

The effect of temperature dependence is shown in Fig. 3. With the rise in temperature, the number of accessible states increases. The steps in the current round off [case (a)], and the amplitude of the oscillations in the conductance vs voltage curve [case (b)] decreases. The peaks in the JMR [case (c)] and the DJMR vs voltage curves [case (d)] become broader and reduced in size.

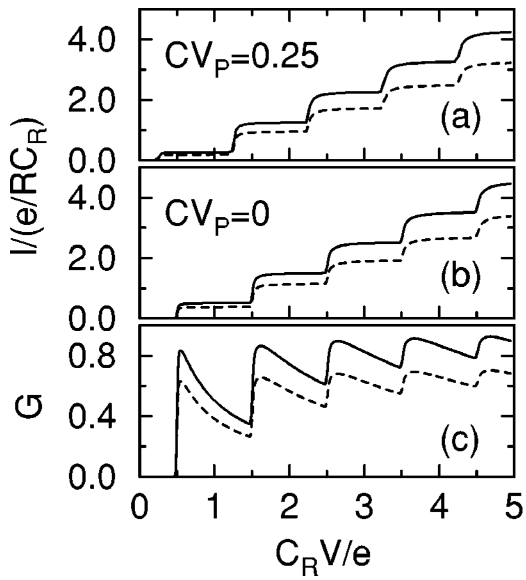

FIG. 2. Current (I) and total conductance (G) as a function of voltage, for a FM/I/FM/I/FM tunnel junction. For cases (a), (b), and (c), the solid lines represent the current and the conductance for parallel alignment of the magnetizations, whereas the dashed lines are for antiparallel alignment. As a function of voltage the current shows steps [cases (a) and (b)], and the total conductance oscillates with decreasing amplitudes [case (c)]. Case (a) corresponds to finite offset voltage $CV_P=0.25$. Cases (b) and (c) are for zero offset voltage. The effect of a finite offset voltage is to shift the position of the I-V curves. We choose the left and the center metals to be made of iron with polarization $P_{\mathrm{Fe}}=0.40$, the right metal to be made of cobalt with polarization $P_{\mathrm{Co}}=0.34$ (Ref. 2). The different parameters used are $C_{\mathrm{L}}=0.01C$, $R_{\mathrm{L}}^{\mathrm{P}}=0.01(R_L^{\mathrm{P}}+R_R^{\mathrm{P}})$, and $k_BT=0.01E_C$.

Restricting ourselves to $k_BT<<E_C$ and zero offset voltage $(CV_P=0)$, in Fig. 4 we plot the junction magnetoresistance for four different cases: (a) $\mathrm{FM_1/I/FM_1/I/FM_2}$, (b) $\mathrm{FM_2/I/FM_1/I/FM_1}$, (c) $\mathrm{FM_1/I/FM_1/I/PM}$, and (d) $\mathrm{PM/I/FM_1/I/FM_1}$, where $\mathrm{FM_1}$ and $\mathrm{FM_2}$ are different ferromagnets. In the high-bias regime for all four cases, the current is linearly proportional to the voltage,[39]

$$I=\frac{e}{(R_L+R_R)C}\left[\frac{CV}{e}-1\right]. \tag{15}$$

It then follows from Eq. (15) that the plateaus in Figs. 4(a)–4(d) are given by the difference in the total resistances from antiparallel to parallel alignments divided by the total resistance for the antiparallel alignment,

$$\mathrm{JMR(plateau)}=1-\frac{R_L^{\mathrm{P}}+R_R^{\mathrm{P}}}{R_L^{\mathrm{AP}}+R_R^{\mathrm{AP}}}. \tag{16}$$

For asymmetric junctions in the low-voltage, low-temperature regime we see spikes in the JMR vs voltage curves in Fig. 4. The occurrence of the first spike can be understood analytically. We confine ourselves to only three states: the $n=0$ state and the two states $n=\pm 1$ immediately

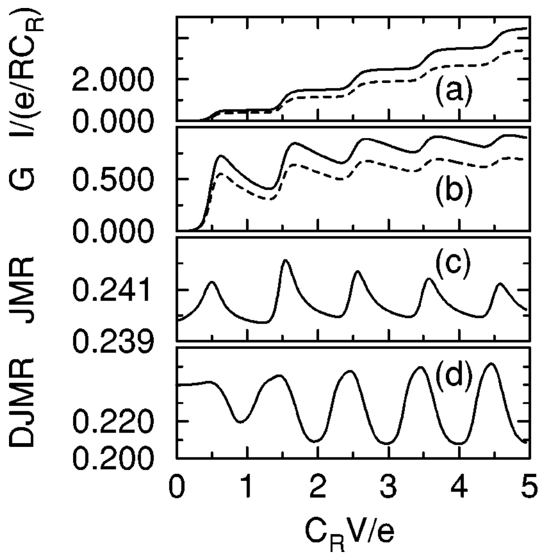

FIG. 3. Temperature dependence of the (a) current, (b) conductances, (c) JMR, and (d) DJMR for a FM/I/FM/I/FM tunnel junction. As in Fig. 2, the solid and the dashed lines represent the current and the conductance for parallel and antiparallel alignments. With increase in temperature, the steps in the current vs voltage curve round off [case (a)], resulting in reduced amplitude of oscillations in the total conductance [case (b)]. The peaks in both the JMR [case (c)] and the DJMR [case (d)] curves broaden. Also the peaks in the JMR and the DJMR curves decrease with an increase in temperature. The parameters are the same as used in Fig. 2, except for the temperature which is $k_BT=0.1E_C$.

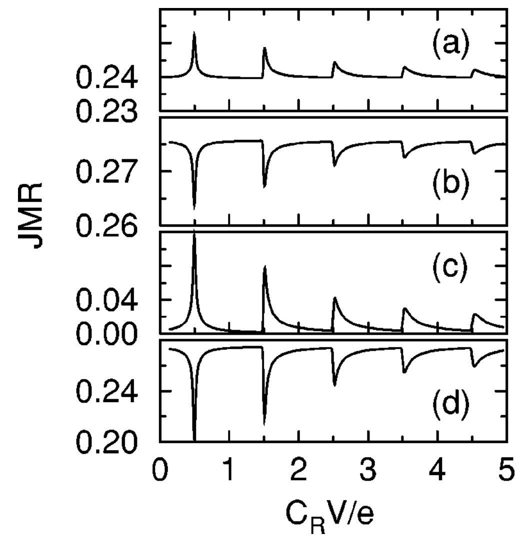

FIG. 4. Junction magnetoresistance as a function of voltage for different cases: (a) $FM_1/I/FM_1/I/FM_2$, (b) $FM_2/I/FM_1/I/FM_1$, (c) $FM_1/I/FM_1/I/PM$, and (d) $PM/I/FM_1/I/FM_1$, where FM_1 and FM_2 are two different ferromagnets, and PM is any paramagnet. In all cases we see spikes in the JMR: spikes go up for cases (a) and (c) whereas spikes go down for cases (b) and (d). These spikes occur at those places where the current increases by a step [see Fig. 2(b)]. The plateaus in all cases are given by the difference in the total resistances from antiparallel to parallel alignments divided by the total resistance for the antiparallel alignment. As a function of voltage the variation of JMR is larger when one of the end metals is a paramagnet [cases (c) and (d)]. For our plots we consider the ferromagnet FM_1 to be of iron, and FM_2 is of cobalt. The parameters chosen are the same as in Fig. 2.

accessible from it. At very low temperature, the state which is most likely occupied is the $n=0$ state for $V_P=0$. The tunnel rates $\Gamma_{0\rightarrow1}$ and $\Gamma_{1\rightarrow0}$ do not enter in the expression for the tunneling current at zero temperature, but at finite temperature they do contribute. In the limit of zero temperature, where we replace the function $\gamma(\epsilon)$ in Eq. (3) by $\gamma(\epsilon)=\epsilon\theta(\epsilon)$, the steady state current can be expressed in terms of the tunnel rates in the regime $(e/2)\leqslant C_RV\leqslant(C_R/C_L)(e/2)$ as

$$I=e\,\frac{\Gamma^L_{0\rightarrow-1}\Gamma^R_{-1\rightarrow0}}{(\Gamma^L_{0\rightarrow-1}+\Gamma^R_{-1\rightarrow0})}. \tag{17}$$

In the derivation of Eq. (17) we have assumed that the capacitance of the right junction is larger than the capacitance of the left junction, i.e., $C_R>C_L$. Near the special point $C_RV\approx e/2$, where the current increases by a step at zero temperature, the height of the spike is simply given by the difference,

$$\mathrm{JMR}\left(C_RV=\frac{e}{2},T\rightarrow0\right)=1-\frac{R_L^{\mathrm{P}}}{R_L^{\mathrm{AP}}}. \tag{18}$$

However, at finite temperature, the height of the spikes depends on the temperature, the capacitances, and the resistances of the junctions. We also notice that spikes go up for cases 4(a) and 4(c) whereas spikes go down for cases 4(b) and 4(d). Cases 4(a) and 4(b) or cases 4(c) and 4(d) differ only by the exchange of the metals in the left and the right leads. In all the above cases we keep the resistance of the left junction for the parallel alignment fixed, $R_L^{\mathrm{P}}=0.01(R_L^{\mathrm{P}}+R_R^{\mathrm{P}})$. By only exchanging the metals of the left and the right leads, we go from spikes which go up to spikes which go down and vice versa. The interchange of the spikes from up to down or down to up can be explained in the following way. At zero temperature, whenever the JMR obtained from Eq. (18) is greater than the height of the plateau [Eq. (16)], we see an up spike [Figs. 4(a) and 4(c)]: otherwise, we see a down spike [Figs. 4(b) and 4(d)]. Within Julliere's model,[3] we should mention that to see the spikes, the left or the right metal should be of a different ferromagnetic material. When all three metals are of the same ferromagnetic materials, the steady state solution $\rho_n^0(t)$ is the same for parallel and antiparallel orientations of magnetizations since the solution depends only on the ratio of the left and the right resistances.

Comparing Figs. 4(a) and 4(b) with Figs. 4(c) and 4(d), we see that the variation of the JMR as a function of voltage is larger when one of the leads is nonmagnetic. Following Eq. (16) and Eq. (18), which give the height of the plateau and the height of the first spike at zero temperature, we see that the height of the plateau for case 4(c) is lower than for case 4(a). On the other hand, the heights of the first spikes are same for both cases because the metals in the left and the center are same. Thus the variation of the JMR for case 4(c) is more than case 4(a). Cases 4(b) and 4(d) can be understood similarly.

We plot the differential junction magnetoresistance as a function of the voltage in Fig. 5 for the same cases as in Fig. 4 and in the same parameter regime. Many of the features of

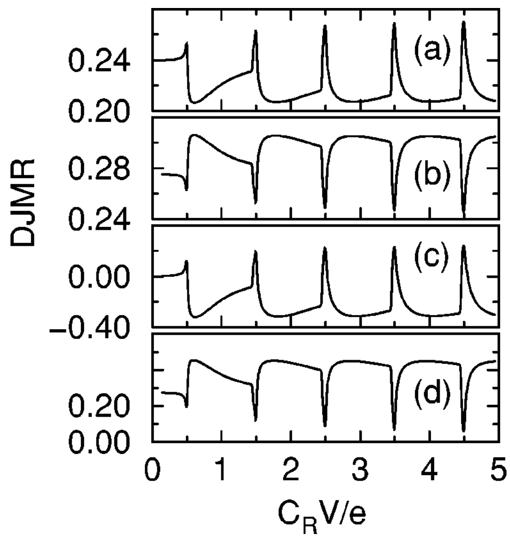

FIG. 5. Differential junction magnetoresistance as a function of voltage for the same cases as in Fig. 4. We see spikes in the DJMR at those places where the current increases by a step. As in Fig. 4, the variation in the DJMR is larger as a function of voltage for cases (c) and (d) compared to cases (a) and (b). For case (c) the DJMR changes sign. Also compared to Fig. 4, the change in the DJMR is larger than the JMR. The metals are the same as used in Fig. 4 and the parameters are identical to Fig. 2.

the DJMR are the same as for the JMR. The spikes are at the same places. The height of the spikes is also the same as in Eq. (18). The DJMR at large voltages is obtained from the classical value with two resistors in series. Finally, the variation of the DJMR with the voltage is larger in cases 5(c) and 5(d) than in cases 5(a) and 5(b). There are, however, some differences. The DJMR can be negative, as shown in Fig. 5(c), while the JMR must be positive from Eq. (18) as long as $R_L^{\mathrm{P}}<R_L^{\mathrm{AP}}$ and $C_R>C_L$. Also, comparing Fig. 4 with Fig. 5, we see that the variation of the DJMR as a function of voltage is larger than the variation of the JMR with the voltage.

IV. CONCLUSION

In this paper we have computed the junction magnetoresistance and the differential junction magnetoresistance for double tunnel junctions with magnetic metals in the Coulomb blockade regime. As expected in a Coulomb blockade problem, the steps in the current and the oscillations in the total conductance are observed for both the parallel and antiparallel orientations of the magnetizations, and the structure is reduced with increasing temperature.

The JMR as a function of voltage shows spikes at the same places where the current increases by a step. The height of the spikes in general depends on the temperature, capacitances, and the resistances of the system whereas the height of the plateaus in the JMR vs voltage curves is given by the classical value obtained by adding two resistors in series. For asymmetric junctions where $C_R>C_L$, the spikes go up if the ratio of the resistances of the right junction for parallel and antiparallel alignments $(R_R^{\mathrm{P}}/R_R^{\mathrm{AP}})$ is greater than the same ratio of the resistances of the left junction $(R_L^{\mathrm{P}}/R_L^{\mathrm{AP}})$. Otherwise, the spikes go down.

Many of the features of the DJMR are similar to the JMR: the spikes occur at the same places, the height of the first spike at zero temperature is the same, and the signs (up or down) of the spikes are the same. Also at high bias, the DJMR saturates to the classical value obtained by adding two resistors in series. However, there are a few differences. The DJMR can be negative for some cases, while the JMR is positive as long as $R_L^{\mathrm{P}}<R_L^{\mathrm{AP}}$ and $C_R>C_L$. Finally, the variation of the DJMR is larger as a function of voltage than that of the JMR.

In conclusion, double-tunnel-junction systems which have magnetic metals exhibit rich Coulomb blockade conductance vs voltage curves. These curves provide a signature of both the Coulomb charging effects and the spin polarization of the tunneling. By measuring the JMR or DJMR, one can extract information about both the capacitance charging energies and the spin polarization of the tunneling electrons, testing both theories of spin-polarized tunneling and the Coulomb blockade. Furthermore, there are cases where the JMR can be dramatically enhanced near one of the Coulomb blockade steps, meaning that there may be some applications of these effects. In any case, for small enough systems, both charging and spin polarization effects will be important.

ACKNOWLEDGMENTS

This work was supported by DOD and AFOSR Grant No. F49620-96-1-0026, and NSF Grant No. DMR9357474, and the NHMFL. We would like to thank J. Chen for useful discussions.

[1] E. L. Wolf, *Principles of Tunneling Spectroscopy* (Clarendon Press, New York, 1969).
[2] P. M. Tedrow and R. Meservey, Phys. Rep. **238**, 1714 (1994).
[3] M. Julliere, Phys. Lett. **54A**, 225 (1975).
[4] C. T. Tanaka, J. Nowak, and J. S. Moodera, J. Appl. Phys. **81**, 5515 (1997).
[5] C. L. Platt, B. Dieny, and A. E. Berkowitz, J. Appl. Phys. **81**, 5523 (1997); Appl. Phys. Lett. **69**, 2291 (1996).
[6] S. Maekawa and U. Gäfvert, IEEE Trans. Magn. **MAG-18**, 707 (1982).
[7] J. Nowak and J. Rauluszkiewicz, J. Magn. Magn. Mater. **109**, 79 (1992).
[8] Y. Suezawa and Y. Gondo, in *Proceedings of the International Symposium on Physics of Magnetic Materials, Sendai* (World Scientific, Singapore, 1987), p. 303; J. Magn. Magn. Mater. **126**, 524 (1993).
[9] R. Nakatani and M. Kitada, J. Mater. Sci. Lett. **10**, 827 (1991).
[10] T. S. Plaskett, P. P. Freitas, N. P. Barradas, M. F. da Silva, and J. C. Soares, J. Appl. Phys. **76**, 6104 (1994).
[11] P. LeClair, J. S. Moodera, and R. Meservey, J. Appl. Phys. **76**, 6546 (1994).
[12] T. Miyazaki, T. Yaoi, and S. Ishio, J. Magn. Magn. Mater. **98**, L7 (1991).

[13] T. Miyazaki and N. Tenuza, J. Magn. Magn. Mater. **139**, L231 (1995).

[14] J. S. Moodera, L. R. Kinder, T. M. Wong, and R. Meservey, Phys. Rev. Lett. **74**, 3273 (1995); J. S. Moodera and L. R. Kinder, J. Appl. Phys. **79**, 4724 (1996).

[15] C. J. Gorter, Physica (Amsterdam) **17**, 777 (1951).

[16] I. O. Kulik and R. I. Shekhter, Zh. Eksp. Teor. Fiz. **68**, 623 (1975) [Sov. Phys. JETP **41**, 308 (1975)].

[17] K. K. Likharev, IBM J. Res. Dev. **32**, 144 (1988).

[18] D. V. Averin and K. K. Likharev, in *Mesoscopic Phenomena in Solids*, edited by B. Altshuler *et al.* (Elsevier, New York, 1991).

[19] G. Schon and A. D. Zaikin, Phys. Rep. **198**, 237 (1990).

[20] *Single Charge Tunneling*, edited by H. Grabert and M. Devoret, Vol. 294 of *NATO Advanced Study Institute, Series B: Physics* (Plenum, New York, 1992).

[21] M. S. Raven, Phys. Rev. B **29**, 6218 (1984) and reference therein.

[22] A. E. Hanna and M. Tinkham, Phys. Rev. B **44**, 5919 (1991).

[23] T. A. Fulton and G. J. Dolan, Phys. Rev. Lett. **59**, 109 (1987).

[24] D. C. Ralph, C. T. Black, and M. Tinkham, Phys. Rev. Lett. **78**, 4087 (1997); **74**, 3241 (1995); C. T. Black, D. C. Ralph, and M. Tinkham, *ibid.* **76**, 688 (1996).

[25] V. Chandrasekhar, Z. Ovadyahu, and R. A. Webb, Phys. Rev. Lett. **67**, 2862 (1991).

[26] S. Gregory, Phys. Rev. Lett. **64**, 689 (1990).

[27] R. Wilkins, E. Ben-Jacob, and R. C. Jaklevic, Phys. Rev. Lett. **63**, 801 (1989).

[28] J. B. Barner and S. T. Ruggiero, Phys. Rev. Lett. **59**, 807 (1987).

[29] L. S. Kuz'min and K. K. Likharev, Pis'ma Zh. Eksp. Teor. Fiz. **45**, 389 (1987) [JETP Lett. **45**, 495 (1987)].

[30] P. J. M. van Bentum, R. T. M. Smokers, and H. van Kempen, Phys. Rev. Lett. **60**, 2543 (1988).

[31] C. W. J. Beenakker, Phys. Rev. B **44**, 1646 (1991).

[32] S. Sankar, B. Dieny, and A. E. Berkowitz, J. Appl. Phys. **81**, 5512 (1997).

[33] R. Wilkins, E. Ben-Jacob, and R. C. Jaklevic, Phys. Rev. Lett. **63**, 801 (1989).

[34] J. Lambe and R. C. Jaklevic, Phys. Rev. Lett. **22**, 1371 (1969).

[35] M. Amman, K. Mullen, and E. Ben-Jacob, J. Appl. Phys. **65**, 339 (1989).

[36] K. K. Likharev, IEEE Trans. Magn. **MAG-23**, 1142 (1987).

[37] H. Tamura and S. Hasuo, J. Appl. Phys. **62**, 3036 (1987).

[38] M. Amman, R. Wilkins, E. Ben-Jacob, P. D. Maker, and R. C. Jaklevic, Phys. Rev. B **43**, 1146 (1991).

[39] S. Hershfield, J. H. Davies, P. Hyldgaard, C. J. Stanton, and J. W. Wilkins, Phys. Rev. B **47**, 1967 (1993).

[40] B. Laikhtman, Phys. Rev. B **43**, 2731 (1991).